

# Comparison of the Photocatalytic Behavior of TiO<sub>2</sub> Coatings Elaborated by Different Thermal Spraying Processes

Filofteia-Laura Toma, Dmitry Sokolov, Ghislaine Bertrand, Didier Klein, Christian Coddet, and Cathy Meunier

(Submitted February 21, 2006; in revised form April 12, 2006)

This paper proposes a comparative study on the microstructure and photocatalytic performances of titanium dioxide coatings elaborated by various thermal spraying methods (plasma spraying in atmospheric conditions, suspension plasma spraying, and high-velocity oxyfuel spraying). Agglomerated spray dried anatase TiO<sub>2</sub> powder was used as feedstock material for spraying. Morphology and microstructural characteristics of the coatings were studied mainly by scanning electron microscopy and x-ray diffraction. The photocatalytic behavior of the TiO<sub>2</sub>-base surfaces was evaluated from the conversion rate of gaseous nitrogen oxides (NO<sub>x</sub>). It was found that the crystalline structure depended strongly on the technique of thermal spraying deposition. Moreover, a high amount of anatase was suitable for the photocatalytic degradation of the pollutants. Suspension plasma spraying has allowed retention of the original anatase phase and for very reactive TiO<sub>2</sub> surfaces to be obtained for the removal of nitrogen oxides.

**Keywords** high-velocity oxyfuel, nitrogen oxides, photocatalysis, photocatalytic activity, plasma spraying, suspension plasma spraying, titanium dioxide

## 1. Introduction

Titanium dioxide (TiO<sub>2</sub>) is an attractive material for numerous technological processes. It finds applications in heterogeneous catalysis, in solar cells for the production of hydrogen and electric energy, as gas sensor, as pigments in foodstuffs, paints, cosmetics, or pharmacology, as a corrosive-protective coating, in electronic devices as varistors, and so on. After the initial work by Fujishima and Honda (Ref 1) on the photolysis of water on TiO<sub>2</sub> electrodes without an external bias, extensive studies on titania for photoelectrical and photochemical applications have been carried out in the last few decades. As photocatalyst, TiO<sub>2</sub> can be used in the degradation of pollutants from air and water, in the photo-induced superhydrophilicity, in sterilization, and even in cancer therapy (Ref 2-4).

Among different physical and chemical characteristics of titania that have an influence on the photocatalytic performance, the crystalline structure seems to be the most important. It is

generally assumed that the anatase (metastable phase) presents a higher photocatalytic activity than the rutile (stable phase). However, some anatase powders containing small quantities of rutile present a better efficiency than that of pure anatase (Ref 5, 6).

For the photocatalytic applications, TiO<sub>2</sub> can be used in the form of powder or coating deposited by numerous techniques. Generally, the reactivity of the supported titania is lower than that of powder. The studies performed in the last years showed that the technique of thermal spraying can be used to produce titania coatings with an effective photocatalytic performance for the decomposition of organic compounds or nitrogen oxides. By the way, several methods of thermal spraying were developed to obtain active photocatalytic deposits (Ref 7-13).

This paper describes a comparative study on the microstructure and photocatalytic performance of nanostructured TiO<sub>2</sub> coatings elaborated by different techniques of thermal spraying: plasma spraying in atmospheric conditions, suspension plasma spraying, and high-velocity oxyfuel spraying (HVOF). The coatings microstructure was characterized by scanning electron microscopy (SEM) and x-ray diffraction (XRD). The photocatalytic efficiency was evaluated by degradation of gaseous nitrogen oxides pollutants.

## 2. Experimental

### 2.1 Materials

Anatase nanosized TiO<sub>2</sub> powder (ST01, Ishihara Sangyo, Japan, 7 nm) was agglomerated by a spray dried technique (using polyvinyl alcohol as organic binder) to obtain spherical micrometer-sized self-standing granules for thermal spraying. The powder was sieved to obtain a size distribution ranging from 10 to 50 μm (Fig. 1). TiO<sub>2</sub> P25 powder (Degussa AG, Germany) that contains 82 vol.% anatase phase (27 nm grain size) and rutile (50 nm) was used as a material reference for the photocatalytic tests.

This article was originally published in *Building on 100 Years of Success, Proceedings of the 2006 International Thermal Spray Conference* (Seattle, WA), May 15-18, 2006, B.R. Marple, M.M. Hyland, Y.-Ch. Lau, R.S. Lima, and J. Voyer, Ed., ASM International, Materials Park, OH, 2006.

Filofteia-Laura Toma, Dmitry Sokolov, Ghislaine Bertrand, Didier Klein, and Christian Coddet, Laboratoire d'Etudes et de Recherches sur les Matériaux, les Procédés et les Surfaces (LERMPS), Université de Technologie de Belfort-Montbéliard (UTBM), Site de Sévenans, 90010 Belfort Cedex, France; and Cathy Meunier, FEMTO-CREST ST (UMR-CNRS 6000) Pôle Universitaire des Portes du Jura, 25211 Montbéliard, France. Contact e-mail: filofteia-laura.toma@utbm.fr.

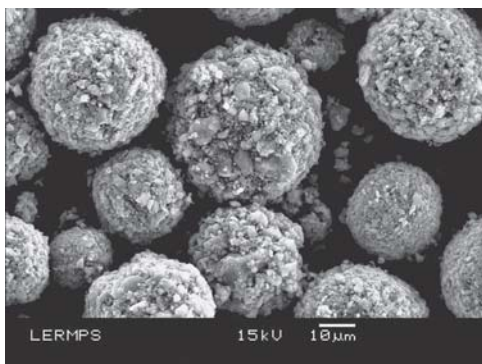


**Fig. 1** SEM morphology of the agglomerated anatase ST01 nanopowder

## 2.2 Thermal Spraying

Different techniques of thermal spraying were used to elaborate nanostructured coatings. Moreover, the spray conditions have been adjusted to minimize the particle heat input and to maintain the original anatase metastable phase in the coating. Plasma spraying in atmospheric conditions (APS) was carried out with a Sulzer-Metco PTF4 plasma gun (6 mm nozzle torch) (Switzerland). The powder at a feed rate of about 14 g/min was carried out by Ar (at 3 L/min flow rate) in the plasma jet obtained from 40 L/min Ar and 3 L/min H<sub>2</sub> plasma gases mixture. The arc current was fixed at 400 A. XC10 (Est Acier, France) mild steel substrates (60 by 70 by 2 mm<sup>3</sup>) previously sand blasted were fixed at 100 mm from exit of the nozzle torch.

Plasma spraying from a powder suspension (technique known as suspension plasma spraying, or SPS) was also used to deposit TiO<sub>2</sub> coatings. A special device was designed to allow the slurry (suspension of fine particles in a solvent) injection in the plasma jet (Ref 13). The aqueous suspension containing 25 wt.% agglomerated powder without any dispersing agent was introduced using a peristaltic pump, at a feed rate of about 25 mL/min, in the system that ensured the atomization of the slurry and radial injection of the resulting drops in the plasma jet. Argon at a flow rate of 5 L/min allowed the fragmentation of the liquid in the enthalpic source. The spraying conditions were similar to that of conventional APS.

The HVOF spraying was performed with a Sulzer-Metco (Winterthur, Switzerland) CDS 100 gun (3 in. nozzle) using natural methane gas, as fuel gas. The flame was obtained by the combustion of 100 L/min CH<sub>4</sub> with 400 L/min O<sub>2</sub>. N<sub>2</sub> at a flow rate of 50 L/min was also added to the gas mixture to decrease the flame temperature. The powder feed rate was 20 g/min and was carried by N<sub>2</sub> at a flow rate of 9.5 L/min. The spray distance was fixed at 150 mm. In the flame, the powder was injected by two different methods: internal injection, that is, as in the conventional HVOF process, and external injection, that is, from outside of the nozzle torch (Ref 14).

## 2.3 Characterization

The coating morphology was examined using a JEOL (Tokyo, Japan) JSM-5800 LV (SEM). X-ray diffraction (X'Pert MPD Philips [Eindhoven, The Netherlands] diffractometer)

with Cu-K $\alpha$  radiation was used to assess the anatase to rutile ratio. Scan step was 0.02° s<sup>-1</sup> with a step time of 0.5 s in the 20 to 90° 2 $\theta$  range. The volume percentage of anatase was determined according to the relation (Ref 15):

$$C_A = \frac{8I_A}{8I_A + 13I_R} \quad (\text{Eq 1})$$

where  $I_A$  and  $I_R$  are the x-ray intensities of the anatase (101) and the rutile (110) peaks, respectively. The crystallite size was evaluated from the XRD based on the Scherrer formula.

The photocatalytic performance of TiO<sub>2</sub> was evaluated by the decrease of nitrogen oxides (NO, NO<sub>x</sub>) concentration in a purpose-built test chamber described elsewhere (Ref 16). The nitrogen oxides, prepared in situ by chemical reaction between copper powder and nitric acid, were introduced in an environmental chamber (about 0.4 m<sup>3</sup> in volume) until the nitrogen oxides concentration reached 1.5 to 2.0 ppm. A fan was also installed to ensure the homogenization of nitrogen oxides concentration in the environmental chamber. The photocatalytic reactor, a polycarbonate box (100 × 100 × 5 mm<sup>3</sup>) equipped with a Plexiglas window, which permits the light passage from a 15 W daylight lamp with a fraction of 30% UVA and 4% UVB, was placed inside the environmental chamber and crossed by the nitrogen oxides flow (the flow rate was 0.6 L/min). The NO and NO<sub>x</sub> concentrations were measured continuously using an AC-30M NO<sub>x</sub> dual chamber with a chemiluminescence analyzer (Environmental SA, France) and recorded with a data acquisition system.

The photocatalytic tests were performed over the sprayed coatings and the powders (agglomerated anatase ST01 and Degussa P25). 0.4 g of each powder were dispersed by mechanical sieving on the surface of a petri dish with an area of about 54 cm<sup>2</sup>. The photocatalytic performance of the powders or the coatings were evaluated as the ratio of the photocatalytic conversion of nitrogen oxides and determined by the relations:

$$\text{NO conversion (\%)} = \frac{[\text{NO}]_{\text{initial}} - [\text{NO}]_{\text{UV}}}{[\text{NO}]_{\text{initial}}} \times 100 \quad (\text{Eq 2})$$

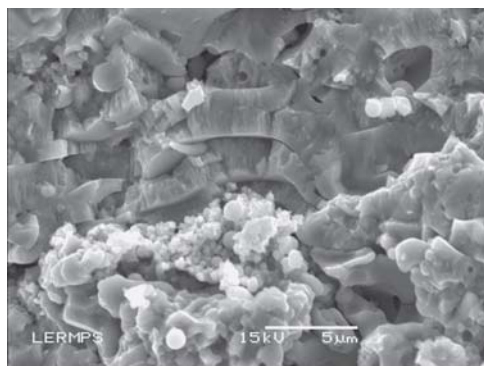
$$\text{NOx conversion (\%)} = \frac{[\text{NOx}]_{\text{initial}} - [\text{NOx}]_{\text{UV}}}{[\text{NOx}]_{\text{initial}}} \times 100$$

where NO conversion (%) and NO<sub>x</sub> conversion (%) are the photocatalytic removal of NO and NO<sub>x</sub> concentrations in the presence of the catalyst and UV irradiation,  $[\text{NO}]_{\text{initial}}$  and  $[\text{NOx}]_{\text{initial}}$  represent the values of the NO and NO<sub>x</sub> concentrations without UV irradiation, and  $[\text{NO}]_{\text{UV}}$  and  $[\text{NOx}]_{\text{UV}}$  are the values of the NO and NO<sub>x</sub> concentrations under UV irradiation.

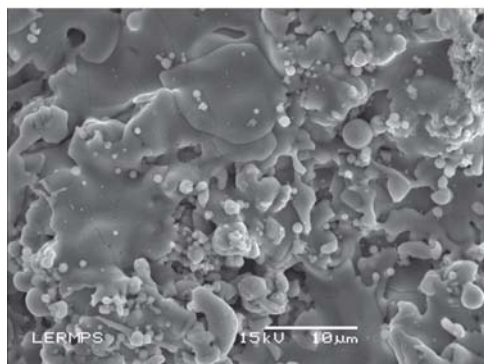
## 3. Results and Discussions

### 3.1 Microstructural Characterization of Coatings

**3.1.1 Plasma Spraying.** The morphology of the plasma sprayed coatings depends on the way each droplet flattens and solidifies at impact on the substrate or on the previously deposited particles (Ref 17). The microstructure of TiO<sub>2</sub> deposits depends on the method of plasma spraying used. Thus, the coating



(a)



(b)

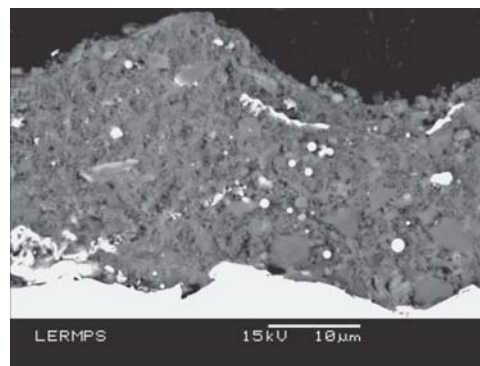
**Fig. 2** SEM morphologies of nanostructured  $\text{TiO}_2$  coating elaborated by conventional atmospheric plasma spraying (APS): (a) fractured cross section; (b) surface

elaborated by conventional plasma spraying was characterized by a bimodal distribution of the structure: on the one hand a thin lamellar morphology commonly observed with sprayed coating and on the other hand a structure of densely agglomerated equiaxed grains (Fig. 2).

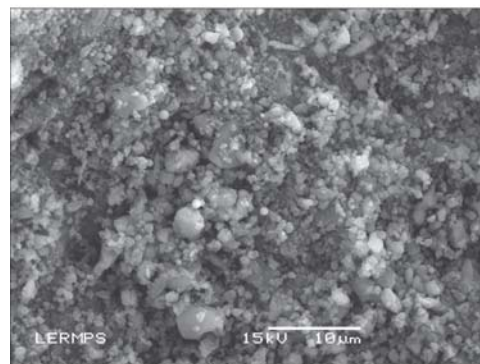
The composite structure of the coating is explained by a relatively large grain-size distribution combined with the temperature heterogeneity of the plasma jet. The lamellas correspond to fully melted particles that passed through the regions where the temperature of the plasma is elevated. In the granular region, partially melted particles anchored in the lamellar structure and unmelted agglomerated particles that almost preserve the spherical morphology were identified (Fig. 2b). These particles crossed the outer zones of the plasma jet where the thermal energy is lower.

The coating prepared by the modified method of APS, using a liquid suspension of the powder as feedstock material (suspension plasma spraying, SPS), did not present the characteristic lamellar microstructure of deposit made by conventional plasma spraying as depicted in Fig. 3. The coating, relatively porous, was constituted of fine partially melted particles as well as “large” particles with a diameter between 2 and 5  $\mu\text{m}$ , which were already observed in the initial agglomerated powder, probably formed during the spray drying process (Fig. 4).

The mechanisms of suspension plasma spraying process were considered to describe the coating formation (Ref 18-20). When the previously atomized liquid suspension is injected in



(a)



(b)

**Fig. 3** SEM images of  $\text{TiO}_2$  coating elaborated by suspension plasma spraying (SPS): (a) cross section; (b) surface

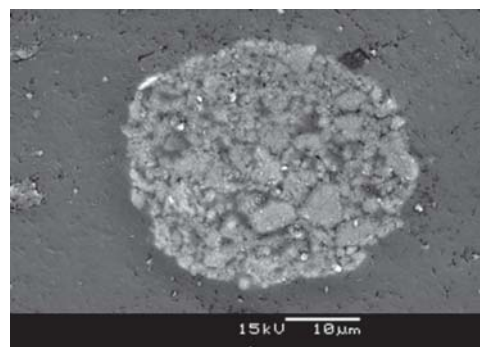
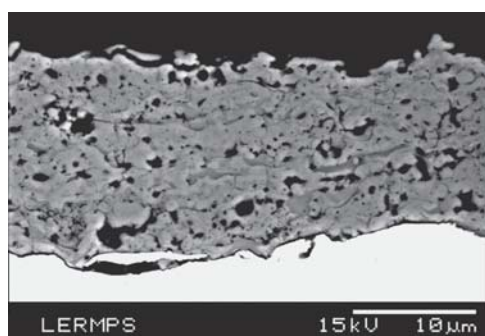


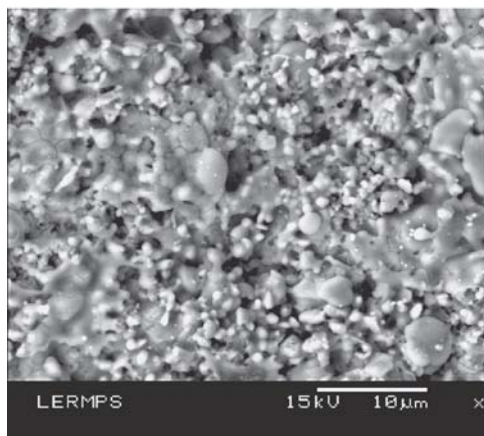
**Fig. 4** View of so-called “large” particles in the initial agglomerated  $\text{TiO}_2$  powder

the plasma, the drops are first disintegrated into smaller ones. Then, the solvent still present in the droplets is evaporated during the plasma crossing and the resulting particles can be heated, melted (or partially melted), and accelerated to the target, thus forming the coating.

**3.1.2 HVOF Spraying.** The morphology of the coatings elaborated by HVOF spraying depended on the manner in which the powder was injected in the flame. The  $\text{TiO}_2$  coating elaborated by conventional HVOF process is porous and characterized by a layered structure that can be observed in most thermally sprayed deposits (Fig. 5). This coating is mainly built up



(a)



(b)

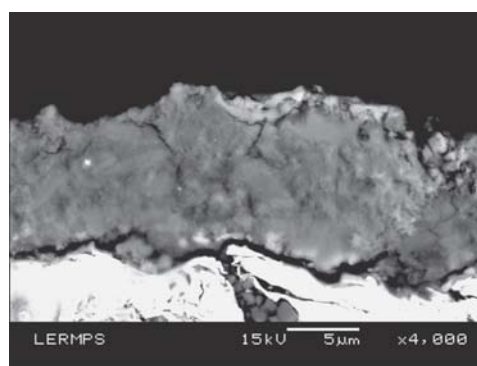
**Fig. 5** SEM microstructures of titania coating obtained by conventional HVOF process (i.e., internal powder injection): (a) cross section; (b) surface

by the melted nanoparticles impacting on the substrate that flatten to form splats. When the powder was radially injected in the flame, outside the nozzle torch (i.e., the external powder injection) the lamellar structure was hardly identified (Fig. 6). The coating contains mainly partially/nonmelted particles that impinge on the substrate to form the deposit. When the external injection of the powder is used, the heat transfer from the flame to  $\text{TiO}_2$  particles is not sufficient to ensure the melting before impacting on substrate.

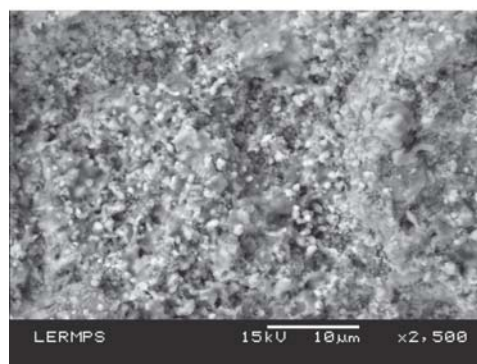
### 3.2 Crystalline Structure in the $\text{TiO}_2$ Coatings

XRD was performed to assess the anatase-to-rutile ratio. The analysis showed that the passage of the feedstock material (as particles or liquid suspension) in the enthalpic source (plasma or flame) involved modifications of the chemical state of titanium dioxide with regard to that of the initial anatase powder. These structural transformations depended on the method of thermal spraying used in the elaboration of the  $\text{TiO}_2$  coatings.

Thus, as depicted in Fig. 7(a), the coating elaborated by plasma spraying contained both anatase (10.9 vol.%, 19.2 nm average size) and rutile (78.6 nm) as well as different titanium suboxides (some  $\text{TiO}_x$  or Magnéli phases). The existence of nonstoichiometric titanium oxides was promoted by the pres-



(a)



(b)

**Fig. 6** SEM microstructures of  $\text{TiO}_2$  deposit prepared by nonconventional HVOF process (i.e., external powder injection): (a) cross section; (b) surface

ence of the hydrogen in the plasma mixture that has a reductive character versus  $\text{TiO}_2$  (Ref 21).

In contrast, in the suspension plasma sprayed coating, only the anatase phase was identified and the crystalline size was preserved (7 nm) identical to the original anatase powder. In this case, the thermal transfer between the plasma and the material was less important than in the case of conventional plasma spraying, because part of the plasma energy was used to vaporize the solvent of the liquid droplets. So, the flight time in the plasma jet was not long enough that the anatase-to-rutile structural transformation occurred before the impact on the substrate.

An important phase transformation was observed in the titania coating obtained by the conventional HVOF process, where only 12.6 vol.% anatase was identified (Fig. 7b). Moreover, the average grains size increased to 80 nm for anatase and 90 nm for rutile. With the modified method of HVOF technique, that is, external powder injection, the structural change was less important, where the anatase content was about 65.6 vol.% with a crystalline size of 18 nm. The rutile grains were around 122 nm.

The crystalline structure of the coating was relative to the melting degree of the particles during spraying. It is generally accepted that the rutile phase correspond to the fully melted particles, whereas the anatase structure was mostly present in the partially and nonmelted particles (Ref 10). Moreover, it was observed that the grain size of rutile phase in all  $\text{TiO}_2$  sprayed coatings was larger than that of anatase regardless of the anatase ratio in the deposits. It was considered that the phase transformation

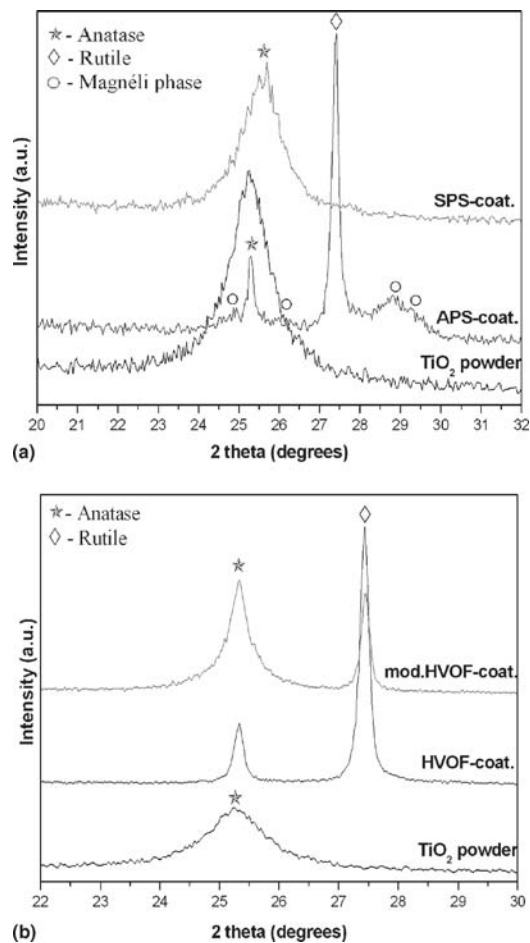


**Fig. 7** XRD patterns of titania coatings elaborated by (a) plasma spraying and suspension plasma spraying and (b) HVOF and modified-HVOF (with external powder injection) processes

from anatase to rutile started at the surface of the nanosized anatase particles (Ref 8, 12) and then increased by nucleation during time in the enthalpic source.

### 3.3 Photocatalytic Properties

The TiO<sub>2</sub> thermal sprayed coatings were tested in the photocatalysis to evaluate their performance versus the nitrogen oxides removal and compared with that of the agglomerated ST01 and P25 powders (Fig. 8). The conversion rate of the pollutants in presence of the ST01 powder was about 31% for NO and 18% for NO<sub>x</sub>, almost similar with that obtained for the reference P25. The photocatalytic responses of the coatings depended on the technique of thermal spraying deposition.

A very low conversion rate of nitrogen oxides pollutants (<5%) was obtained in the presence of the TiO<sub>2</sub> surfaces elaborated by conventional methods of APS and HVOF. The low anatase ratio (<15%) was not sufficient to produce a photocatalytic decrease of nitrogen oxides. Furthermore, it is likely that the anatase phase was embedded in the rutile one. So, this anatase phase cannot be excited by the ultraviolet (UV) light to contribute to the photocatalysis process.

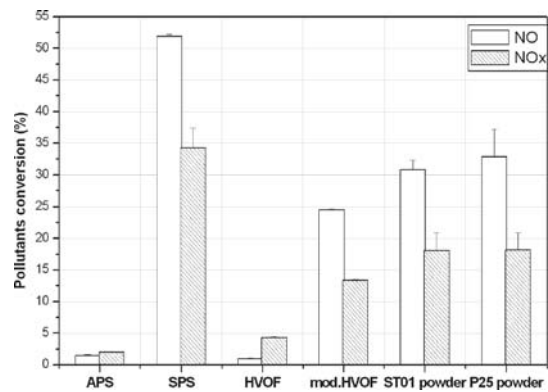


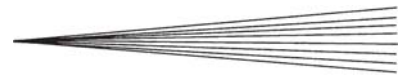
**Fig. 8** Photocatalytic performance of titanium dioxide in the form of powders and thermal sprayed coatings (values of conversion rates after 30 min of UV irradiation)

When the suspension plasma sprayed coating was tested in the photocatalysis, a substantial decrease in the nitrogen oxide concentration was recorded under ultraviolet irradiation: around 52% for NO and 34% for NO<sub>x</sub>. Also, the TiO<sub>2</sub> coating elaborated by modified method of HVOF technique (with an external injection of the agglomerated powder) permitted to remove around 25% NO and 13% NO<sub>x</sub>.

The different photocatalytic activity of the coatings in the nitrogen oxide conversion was principally correlated with the composition of crystalline structure. Anatase phase is a key parameter in the photocatalytic activity, whereas the rutile is less active (Ref 8, 12, 13, 22). A higher anatase content and a reduced size of anatase particles ensured a better decomposition of pollutants (Ref 10, 11, 23). Besides, the titania surface elaborated by suspension plasma spraying provided a higher performance than that of the initial agglomerated powder, although it contained only anatase phase as the feedstock material. In this case, the improvement of the photocatalytic efficiency was attributed to the elimination of powder impurities (such as the organic binder used in the spray drying process) and a cleaning up of the particle surfaces when crossing the plasma. These phenomena may ensure an important activation of the catalytic sites under ultraviolet irradiation.

## 4. Conclusions

This paper proposes a comparative study on the microstructure and photocatalytic properties of titanium dioxide coatings elaborated by different methods of thermal spraying: atmospheric plasma spraying, suspension plasma spraying, HVOF, and a modified method of HVOF with an external injection of feedstock material, starting from an agglomerated TiO<sub>2</sub> anatase nanopowder. The coatings elaborated by conventional techniques of APS and HVOF were characterized by the common lamellar microstructure observed in all thermal sprayed deposits. Moreover, the use of nanoparticles as feedstock material involved the phase transformation anatase to rutile in the enthalpic source. The photocatalytic ability for nitrogen oxides was lower than 5% of that correlated with the reduced anatase ratio.



The coatings elaborated by suspension plasma spraying (SPS) or modified method of HVOF (i.e., with external powder injection) presented a specific structure and a high ratio of partially melted particles. The particles were less heated and structurally transformed in the enthalpic source. With the nonconventional HVOF, an important anatase ratio was observed, while with SPS technique the anatase content and initial crystalline size were preserved. Furthermore, the deposits had a remarkable photocatalytic performance in the nitrogen oxides removal, which in some conditions was higher than that of the initial powder.

The suspension plasma spraying is an interesting technique to produce reactive titania surfaces for the photocatalytic applications. However, surface investigations are still necessary to better clarify the photocatalytic performance of TiO<sub>2</sub> suspension plasma sprayed coatings.

## Acknowledgments

The authors are grateful to Pr. A. Ohmori (Osaka University, Japan) for kindly delivery of agglomerated spray dried TiO<sub>2</sub> anatase powder and to S. Lamy (LERMPS) for performing the microscopic analysis.

## References

1. A. Fujishima and K. Honda, Electrochemical Photolysis of Water at Semiconductor Electrode, *Nature*, 1972, **238**, p 37-38
2. D.F. Ollis and H. Al-Ekabi, *Photocatalytic Purification and Treatment of Water and Air*, Proceeding, Elsevier, 1993
3. A. Mills and S. Le Hunte, An Overview of Semiconductor Photocatalysis, *J. Photochem. Photobiol. A: Photochem.*, 1997, **108**, p 1-35
4. A. Fujishima, T.N. Rao, and D.A. Tryk, Titanium Dioxide Photocatalysis, *J. Photochem. Photobiol. C: Photochem. Rev.*, 2000, **1**, p 1-21
5. D.C. Hurum, A.G. Agrios, K.A. Gray, T. Rajh, and M.C. Thurnauer, Explaining the Enhanced Photocatalytic Activity of Degussa P25 Mixed-Phase TiO<sub>2</sub> Using EPR, *J. Phys. Chem. B*, 2003, **107**, p 4545-4549
6. T. Ohno, K. Tokieda, S. Higashida, and M. Matsumura, Synergism between Rutile and Anatase TiO<sub>2</sub> Particles in Photocatalytic Oxidation of Naphthalene, *Appl. Catal. A: Gen.*, 2004, **244**, p 383-391
7. M. Fukumoto, H. Murayama, and Y.-G. Jung, Fabrication Possibility of Photocatalyst TiO<sub>2</sub> Coating by Thermal Spraying, *Proc. First International Symposium on Environmental Materials and Recycling*, A. Kobayashi, Ed., March 8-9, 2001 (Osaka, Japan), 2001, p 11-16
8. C.-J. Li, G.-J. Yang, and Z. Wang, Effect of Spray Parameters on the Structure of Nano-structured TiO<sub>2</sub> Deposits by Liquid Flame Spray Process, *International Thermal Spray Conference*, ITSC 2002, March 4-6, 2002 (Essen, Germany), E. Lugscheider, Ed., DVS Düsseldorf, 2002, p 544-549
9. F. Ye and A. Ohmori, The Photocatalytic Activity and Photo-Absorption of Plasma Sprayed TiO<sub>2</sub>-Fe<sub>3</sub>O<sub>4</sub> Binary Oxide Coatings, *Surf. Coat. Technol.*, 2003, **160**, p 62-67
10. C. Lee, H. Choi, C. Lee, and H. Kim, Photocatalytic Properties of Nano-Structured TiO<sub>2</sub> Plasma Sprayed Coating, *Surf. Coat. Technol.*, **173**(2-3), 2003, p 192-200
11. G.-J. Yang, C.-J. Li, F. Han, and A. Ohmori, Microstructure and Photocatalytic Performance, of High Velocity Oxy-Fuel Sprayed TiO<sub>2</sub> Coatings, *Thin Solid Films*, 2004, **466**, p 81-85
12. G.-J. Yang, C.-J. Li, and Y.-Y. Wang, Phase Formation of Nano-TiO<sub>2</sub> Particles During Flame Spraying with Liquid Feedstock, *J. Therm. Spray Technol.*, 2005, **14**(4), p 480-486
13. F.L. Toma, G. Bertrand, S.-O. Chwa, C. Meunier, D. Klein, and C. Coddet, Comparative Study on the Photocatalytic Decomposition of Nitrogen Oxides Using TiO<sub>2</sub> Coatings Prepared by Conventional Plasma Spraying and Suspension Plasma Spraying, *Surf. Coat. Technol.*, 2006, **200**(20-21), p 5855-5862
14. F.L. Toma, G. Bertrand, S.O. Chwa, D. Klein, H. Liao, C. Meunier, and C. Coddet, Microstructure and Photocatalytic Properties of Nanostructured TiO<sub>2</sub> and TiO<sub>2</sub>-Al Coatings Elaborated by HVOF Spraying for the Nitrogen Oxides Removal, *Mater. Sci. Eng. A*, 2006, **417**, p 56-62
15. N. Berger-Keller, G. Bertrand, C. Filiatre, C. Meunier, and C. Coddet, Microstructure of Plasma-Sprayed Titania Coatings Deposited from Spray Dried Powder, *Surf. Coat. Technol.*, 2003, **168**, p 281-290
16. F.L. Toma, S. Guessasma, D. Klein, G. Montavon, G. Bertrand, and C. Coddet, Neural Computation to Predict TiO<sub>2</sub> Photocatalytic Efficiency for Nitrogen Oxides Removal, *J. Photochem. Photobiol. A: Chem.*, 2005, **165**, p 91-96
17. R. McPherson, The Relationship between the Mechanism of Formation, Microstructure and Properties of Plasma-Sprayed Coatings, *Thin Solid Films*, 1981, **83**, p 297-310
18. K. Wittmann, F. Blein, J. Fazilleau, J.-F. Coudert, and P. Fauchais, A New Process to Deposit Thin Coatings by Injecting Nanoparticles Suspensions in a DC Plasma Jet, *International Thermal Spray Conference*, ITSC 2002, March 4-6, 2002 (Essen, Germany), E. Lugscheider, Ed., DVS Düsseldorf, 2002, p 519-522
19. C. Delbos, J. Fazilleau, V. Rat, J.F. Coudert, P. Fauchais, and L. Bianchi, Influence of Powder Size Distribution and Heat Flux on Yttria Stabilised Coatings Elaborated by Liquid Suspension Injection in a DC Plasma Jet, *Thermal Spray Connects. Explore Its Surfacing Potential!* May 2-4, 2005 (Basel, Switzerland), E. Lugscheider, Ed., DVS, 2005, CD-Rom version
20. F.L. Toma, G. Bertrand, R. Rampon, D. Klein, C. Coddet, and C. Meunier, Relationship between the Suspensions Properties and Liquid Plasma Sprayed Coatings Characteristics, *International Thermal Spray Conference & Exposition*, May 15-18, 2006 (Seattle, WA), B.R. Marple, M.M. Hyland, Y.-Ch. Lau, R.S. Lima, and J. Voyer, Ed., ASM International, 2006
21. L.M. Berger, Titanium Oxide—New Opportunities for an Established Coating Material, *Thermal Spray Solutions: Advances in Technology and Application*, May 10-12, 2004 (Osaka, Japan), DVS-Verlag, CD-Rom version
22. F.L. Toma, G. Bertrand, D. Klein, and C. Coddet, Photocatalytic Removal of Nitrogen Oxides via Titanium Dioxide, *Environ. Chem. Lett.*, 2004, **2**(3), p 117-121
23. M. Anpo, T. Shima, S. Kodama, and Y. Kubokawa, Photocatalytic Hydrogenation of CH<sub>3</sub>CCH with H<sub>2</sub>O on Small-Particle TiO<sub>2</sub>: Size Quantization Effects and Reaction Intermediates, *J. Phys. Chem.*, 1987, **91**(16), p 4305-4310